Molecular-bond hardening and dynamics of molecular stabilization and trapping in intense laser pulses

Guanhua Yao and Shih-I Chu
Department of Chemistry, University of Kansas, Lawrence, Kansas 66045
(Received 14 October 1992; revised manuscript received 9 March 1993)

We extend our previous study [Chem. Phys. Lett. **197**, 413 (1992)] of the molecular stabilization in intense laser fields by considering the dynamical behavior of the H_2^+ molecules in intense femtosecond short laser pulses at 775 nm. Significant stabilization and population trapping of high-lying vibrational states and chemical bond hardening are predicted for both continuous-wave (cw) lasers and short laser pulses. While the intensity dependences of the laser-induced stabilization are essentially the same for both cases, the detailed wave-packet localization dynamics is quite different. The correlation of the time-dependent dynamics with the time-independent Floquet complex quasienergy results, the probability for localization, the pulse-width dependence of molecular stabilization, the proton kinetic-energy spectrum, as well as the contrary dynamical response of low- and high-lying states, are studied at length for intense short laser pulses. In addition, the dynamic origin of "bond-softening" (for low-lying vibrational states) and "bond-hardening" (for high-lying vibrational states) effects in intense laser fields are explored.

PACS number(s): 34.50.Rk, 33.80.Gj, 33.80.Wz

I. INTRODUCTION

It is now well known that multiphoton dissociation (MPD) of polyatomic molecules is a rather efficient process and can occur in relatively weak infrared laser fields [1,2]. On the other hand, MPD of small molecules such as triatomic and diatomic molecules is a slow and inefficient process, due to the low density and anharmonicity of vibrational states. For diatomic molecules, the nonperturbative time-independent Floquet method and complex vibrational quasienergy formalism [3] was first developed in 1981 and applied to the study of intense-field photodissociation of low-lying vibrational states of H_2^+ for intensity up to 5.0×10^{13} W/cm^2. The laser-intensity-dependent multiphoton excitation dynamics can be understood in terms of the avoided crossings of adiabatic electronic-field potential curves [3]. Subsequently the Floquet method and an inhomogeneous differential equation method were extended for the studies of MPD of H_2^+ [4] and HD^+ [5] from highly excited vibrational states. These latter studies were prompted by the first experimental observation of two-photon dissociation of HD^+ from highly excited vibrational states [6]. These theoretical investigations revealed that MPD from the (weaker-bound) high-lying vibrational levels is far more efficient than from those (tighter-bound) low-lying levels when the intensity of the laser fields is relatively weak. Other related theoretical study using different theoretical methods has postulated the existence of laser-induced bound states for the Ar_2^+ system at a laser intensity around 10^{11} W/cm^2 [7]. All of these earlier theoretical works, however, were confined to the case of continuous-wave (cw) laser excitation. Wave-packet dynamics, laser-pulse effects, and laser-induced bond-softening and bond-hardening effects (the subject of the present paper) were not explored in these studies.

Recent advances in high-intensity experiments on multiphoton and above-threshold ionization of atoms [8] have stimulated renewed interest in the study of multiphoton dynamics in diatomic molecules [9–15]. In particular, experiments on multiphoton dissociation of molecular hydrogen [9–12] have revealed two notable intense-field phenomena. (i) The molecules can absorb more photons than necessary to dissociate the chemical bond, and the kinetic-energy distribution of the dissociated fragments shows the appearance of equally spaced multiple peaks, a phenomenon termed above-threshold dissociation (ATD) [9,13]. (ii) The H_2^+ chemical bond can be "softened" in the presence of intense laser fields, leading to efficient photodissociation of low-lying vibrational levels [9]. The presence of additional internuclear degrees of freedom in molecules enriches greatly the nonlinear multiphoton dynamics.

In a recent letter [14], we investigated the laser-induced resonance structure and multiphoton dynamics of H_2^+ molecules in intense monochromatic fields and reported a high-intensity phenomenon: the "hardening" of molecular bonds and laser-induced stabilization and population trapping of molecules in intense laser fields. In the presence of external electromagnetic fields, all vibrational levels of H_2^+ molecules in the ground ($1s\sigma_g$) electronic state become coupled to the dissociative continuum of the upper (repulsive) electronic state $2p\sigma_u$. As a result, all vibrational levels now turn to (shifted and broadened) quasibound resonance states, which we shall call the *vibrational quasienergy resonances* below. Each vibrational quasienergy resonance state possesses an intensity- and frequency-dependent complex energy ei-

 ©1993 The American Physical Society

genvalue $(E_R, -\Gamma/2)$, the real part of which is related to the ac Stark shift and the imaginary part (width) is relevant to the MPD-ATD rate [3]. We have determined for the first time all the complex vibrational quasienergies of H_2^+ molecules via a recently developed complex-scaling Fourier-grid Hamiltonian (CSFGH) method [15,16] within the complex vibrational quasienergy formalism [3]. The method is simple to implement and allows accurate and efficient determination of both low-lying and highly excited vibrational quasienergy resonances simultaneously by a single diagonalization of a non-Hermitian time-independent Floquet Hamiltonian.

Our Floquet results [14] show that with increasing the laser field strength the high-lying vibrational states are stabilized, in contrast to the low-lying states which become less and less stable ("bond softening" [9]). The lifetimes of these high-lying resonances increase with the laser intensity and the molecular bond is thus harder to break in high fields (which we refer to as "bond hardening"). In addition to the time-independent Floquet calculations, we also performed a time-dependent MPD-ATD dynamical calculation [14] for the case of continuous-wave laser fields with a smooth turning-on ($\sin^2$) ramp. The time-dependent results are in complete consistency with the time-independent Floquet calculations in the prediction of laser-induced trapping and stabilization of high-lying vibrational states.

However, several questions remain open concerning the feasibility of laser-induced stabilization phenomenon under the irradiation of realistic short-pulse high-intensity laser fields. (i) Can the molecules survive the rising part of the laser pulses before they enter the "stabilized" regime? (ii) How is the intrinsic bond-hardening phenomenon manifested and what is the peak-intensity dependence of the molecular stabilization phenomenon under intense short-pulse conditions? (iii) What is the effect of initial preparation of vibrational states and the pulse width on the trapping dynamics? This study is particularly timely, as experimental studies of MPD-ATD dynamics using intense short-pulse laser fields are being pursued in several laboratories. After we finished this work, we became aware of a related theoretical study on wave-packet and vibrational trapping dynamics in H_2^+ (at different wavelengths and field strengths and for different pulse shape) that was performed by Giusti-Suzor and Mies [17], using a different theoretical technique.

In this paper, we will extend the previous work and address these questions by studying the MPD-ATD dynamics of the H_2^+ molecular ions in intense Gaussian laser pulses. The peak-intensity dependence of the stabilization and trapping dynamics and the correlation between the MPD-ATD dynamics and the complex vibrational quasienergies will be focused. In Sec. II we first outline briefly both the time-independent and the time-dependent theoretical frameworks. The molecular vibrational resonance structure and the wave-packet dynamics are studied for cw laser fields. In Sec. III the dynamics of the vibrationally excited molecular ions in intense Gaussian laser pulses is studied in detail for various laser peak intensities, laser-pulse widths, and initial vibrational preparation. This is followed by a conclusion in Sec. IV.

II. MOLECULAR STABILIZATION AND TRAPPING IN cw LASER FIELDS

As the time scales we will consider are much shorter than the rotational time scales (500 fs or longer), the rotational degrees of freedom are frozen and are not involved. We will thus focus our study on the multiphoton excitation of the vibrational degrees of freedom between the two lowest electronic states ($1s\sigma_g$ and $2p\sigma_u$) of the H_2^+ molecular ion. We first discuss the case of continuous-wave laser excitation. In an intense cw laser field, the two electronic states are strongly coupled and a time-independent coupled-channel Floquet approach [3] can be employed to determine the laser-induced vibrational quasienergies.

Recently a CSFGH method has been developed [16] and applied to the study of both shape resonances and MPD-ATD rate [14,15]. The method is simple to implement and allows efficient and accurate determination of the complex vibrational quasienergies $(E_R, -\Gamma/2)$ of both low-lying and high-lying excited states without the need of computing potential matrix elements and imposing any boundary conditions.

Let us consider the response of the H_2^+ (with $\mathbf{r}$ and $\mathbf{R}$ being, respectively, the electronic and the internuclear coordinates) in a laser pulse. The Hamiltonian of the perturbed molecular system is given by

$$\hat{H}(\mathbf{r},\mathbf{R},t)=\hat{T}_R+\hat{H}_{\rm el}(\mathbf{r},\mathbf{R})+\boldsymbol{\mu}(\mathbf{r},\mathbf{R})\cdot\mathbf{E}_0 f(t)\sin\omega t \ , \tag{1}$$

where $\hat{T}_R$ is the nuclear kinetic-energy operator, $\hat{H}_{\rm el}(\mathbf{r},\mathbf{R})$ is the electronic Hamiltonian, $\boldsymbol{\mu}(\mathbf{r},\mathbf{R})$ is the dipole moment operator, $\mathbf{E}_0$ is the field amplitude of the laser pulse with pulse shape $f(t)$. The Schrödinger equation under the Born-Oppenheimer approximation can be reduced to (assuming $\mathbf{E}_0$ is parallel to $\mathbf{R}$)

$$\frac{i\partial}{\partial t}\psi_g(R,t)=[\hat{T}_R+\hat{U}_1(R)]\psi_g+\mu(R)E_0 f(t)\sin(\omega t)\psi_u \ , \tag{2}$$

$$\frac{i\partial}{\partial t}\psi_u(R,t)=[\hat{T}_R+\hat{U}_2(R)]\psi_u+\mu(R)E_0 f(t)\sin(\omega t)\psi_g \ , \tag{3}$$

where $\psi_g(R,t)$ and $\psi_\mu(R,t)$ are the probability amplitudes at internuclear distance R with the electron being in the $1s\sigma_g$ and $2p\sigma_u$ states, respectively, $\hat{U}_1(R)$ and $\hat{U}_2(R)$ are the corresponding internuclear potentials, and $\mu(R)$ is the transition dipole moment between the two electronic states. For the present study, we shall use the velocity gauge for the laser-molecular interaction. As demonstrated in the previous study [15], for weak to medium strong fields, the length and velocity gauges give rise to the same results for complex vibrational quasienergies $(E_R, -\Gamma/2)$. Thus the restriction to the two electronic states in the present study using the velocity gauge is justified. Several authors have recently advocated the use of velocity gauge in strong fields [13(b),15]. This is due to the fact that the use of the velocity gauge leads to vanishing dipolar interaction at large separation R, allowing the reduction of the number of Floquet coupled

channels in strong-field calculations.

In the case of $f(t)=1$, i.e., when the perturbation is periodic in time, Eqs. (2) and (3) can be transformed into an equivalent time-independent infinite-dimensional Floquet Hamiltonian ($\hat{H}_F$) eigenvalue problem [14,15,18]. To determine the complex vibrational quasienergy states, a complex-scaling transformation [18], $R \rightarrow Re^{i\theta}$ can be made which leads to a complex-scaling Floquet Hamiltonian $\hat{H}_F(Re^{i\theta})$. Instead of expanding the nuclear wave functions in terms of a set of basis functions (L^2 basis-set expansion method) as in earlier work [3,4], we can discretize the Floquet Hamiltonian using the Fourier-grid method [19]. The matrix elements in the Floquet basis $|\alpha,n\rangle \equiv |\alpha\rangle \otimes |n\rangle$ (where $|\alpha\rangle$ denotes the electronic states and n is the photon Fourier index ranging from $-\infty$ to $+\infty$) can be written as [14,15]

$$\langle R_i|[\hat{H}_F(\mathrm{R}e^{i\theta})]_{\alpha n,\beta m}|R_j\rangle = \{e^{-2i\theta}\langle R_i|\hat{T}_R|R_j\rangle \Delta R + [U_\alpha(R_i e^{i\theta}) + n\hbar\omega]\delta_{ij}\} \times \delta_{\alpha\beta}\delta_{nm} + \tfrac{1}{2}\mu(R_i e^{i\theta})E_0\delta_{ij}\delta_{n,m\pm1}(1-\delta_{\alpha\beta}) , \quad (4)$$

where

$$\langle R_i|\hat{T}_R|R_j\rangle = (1/N\Delta R)\sum_{l=-L}^{L}(k_l^2/2\mu)\exp[ik_l(R_i-R_j)] , \quad (5)$$

with N being the number of grid points, $R_j = j\Delta R$ ($j=1,2,\ldots,N$), $k_l = l\Delta k = 2\pi l/N\Delta R$, and $L=(N-1)/2$. The desired complex energies are then identified by the stationary points of the θ trajectory of the complex eigenvalues of the non-Hermitian Floquet Hamiltonian $\hat{H}_F(\theta)$. The real parts of the complex energies correspond to the energies of the shifted vibrational states in the laser field and the imaginary parts to the (half) widths (MPD-ATD rates) of the vibrational resonances.

Figs. 1(a)–1(c) display the adiabatic electronic-field potential-energy curves at various laser intensities: (a) $I=10^{11}$ W/cm^2, (b) $I=5\times10^{12}$ W/cm^2, and (c) $I=5\times10^{13}$ W/cm^2. These adiabatic potential curves are obtained by diagonalizing the electronic-plus-field Hamiltonian (the Floquet Hamiltonian $\hat{H}_F$ excluding the nuclear kinetic-energy operator). The wavelength $\lambda=775$ nm will be considered throughout the paper, as a most recent MPD-ATD experiment is performed around it [20]. Each adiabatic curve is labeled asymptotically by the Floquet index $|g$ (or $u),n\rangle$. The line segments at the left-side column represent the real parts of the complex energies of the vibrational resonances. The line segments at the right columns denote the energy levels supported merely by their corresponding adiabatic potential surface. It is seen that while the vibrational level structure is hardly changed at weak intensity ($I=10^{11}$ W/cm^2 or less), the potential curves together with the vibrational level structure are strongly deformed at high fields. In particular, two or more groups of vibrational resonances are formed which are separated from each other. A close comparison between the quasienergy resonances at the left column and the adiabatic levels at the right columns shows they have almost the same energies. This implies that these resonances are closely associated with the formation of the corresponding adiabatic potential wells. The imaginary parts (the half-widths) of the corresponding complex energies are displayed in Figs. 2(a)–2(c). Note particularly the intensity dependence of the rates of the high-lying resonances. Rapid reduction of the widths (rates) with laser intensity is observed for these high-lying resonances. In particular, the widths can be as small as 10^{-10} a.u. (or the photodissociation lifetimes as long as 1 ns) at $I=5\times10^{13}$ W/cm^2. Therefore we find that these high-lying vibrational resonance states are more stable against dissociation at high intensities than at low intensities, an unexpected high-field effect which may be termed as molecular-bond hardening, a manifestation of the laser-induced stabilization phenomenon. The stabiliza-

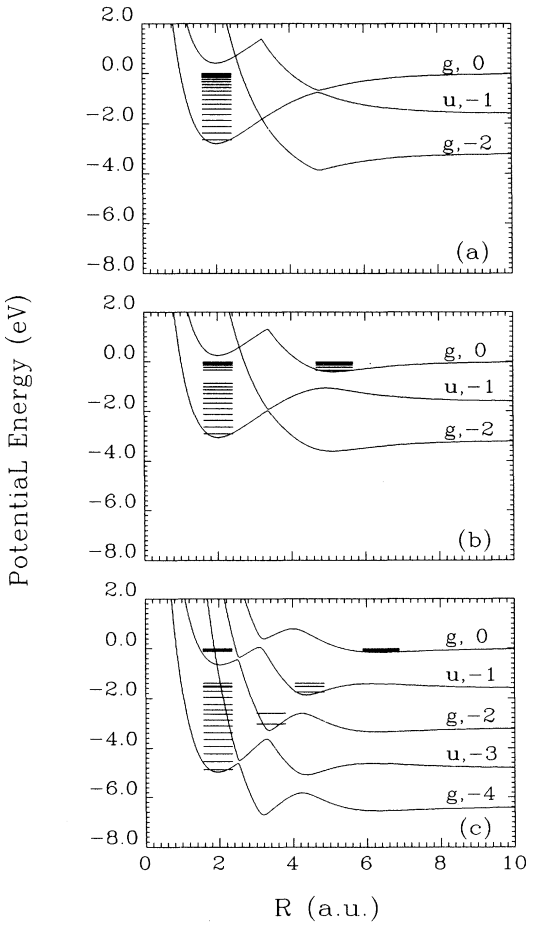

FIG. 1. Vibrational quasienergy-level structure and dressed adiabatic potentials of H_2^+ in the 775-nm laser fields for laser intensity I=(a) 10^{11} W/cm^2, (b) 5×10^{12} W/cm^2, and (c) 5×10^{13} W/cm^2. The line segments at the left column correspond to the energies of the complex quasienergy states, and the line segments at the right columns represent the energy levels supported merely by the corresponding adiabatic potential wells. Each adiabatic potential curve is labeled asymptotically by the Floquet channel index $|g(\text{or } u),n\rangle$.

tion phenomenon is evidently due to the trapping of molecules in various adiabatic potential wells. It is instructive to see that molecules may be trapped at several stretched internuclear separations corresponding to single or multiphoton resonance avoided crossing regimes.

For a general pulse shape $f(t)$ whose temporal dependency is nonperiodic, the non-Hermitian time-independent Floquet formalism for complex energies is not directly applicable. The time-dependent Schrödinger equation, Eqs. (2) and (3), must be directly integrated. The "split-operator" technique [21] is convenient for this purpose. The short-time propagator for the time-dependent Hamiltonian given in Eq. (1) can be written as

$$\hat{U}(t_{j+1},t_j)=e^{-i(\Delta t/2)\hat{T}}e^{-i\hat{V}(t_j+\Delta t/2,R)\Delta t}e^{-i(\Delta t/2)\hat{T}}. \quad (6)$$

For the coupled-channel problem considered here, $\hat{T}$ and $\hat{V}$ are themselves 2×2 block matrices,

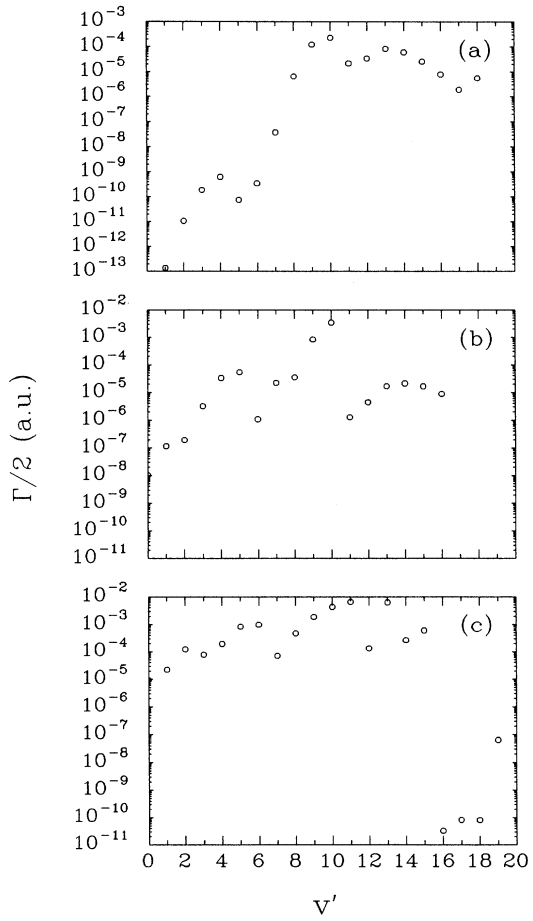

FIG. 2. Multiphoton dissociation (half) widths ($\Gamma/2$) of all the vibrational quasienergy resonance states for the laser intensities considered in Fig. 1, showing the rapid reduction of the photodissociation rates of the high-lying resonances with the laser intensity. Here v' labels the order of quasienergy resonance according to the magnitude of their energies.

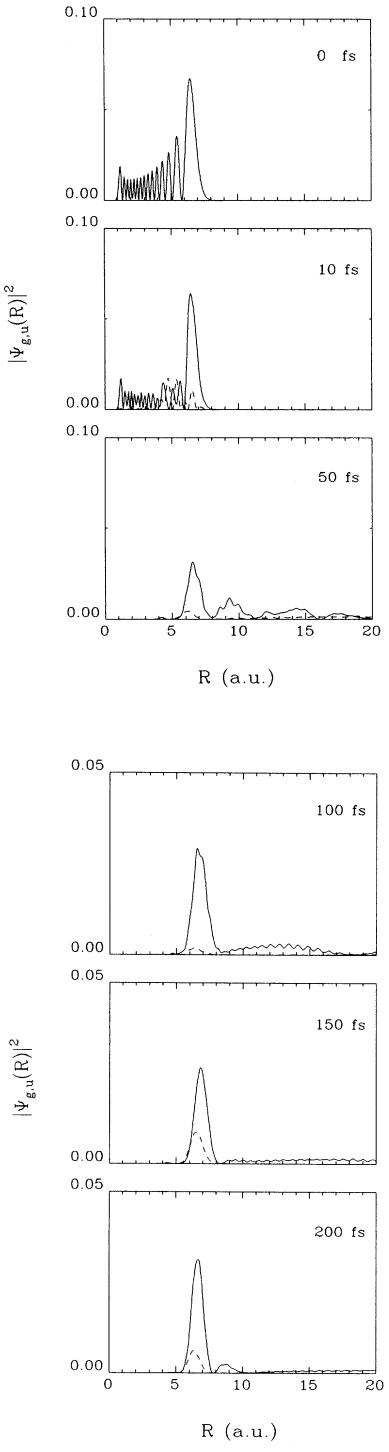

FIG. 3. Time evolution of the molecular wave packet in intense cw-like laser field. The solid line and the dashed line denote, respectively, the wave functions in the $1s\sigma_g$ and the $2p\sigma_u$ electronic states. The molecule is prepared initially at the $v=14$ vibrational state and the laser intensity is 5×10^{13} W/cm^2. A considerable portion of the wave packet is stably localized and trapped for a long period of time at a fixed internuclear distance $R\approx 6.5$ a.u.

$$\hat{T}=\begin{bmatrix}\hat{T}_R & 0\\ 0 & \hat{T}_R\end{bmatrix}, \quad \hat{V}(t,R)=\begin{bmatrix}U_1(R) & D(R,t)\\ D(R,t) & U_2(R)\end{bmatrix}, \tag{7}$$

where $D(R,t)$ is the electric dipole coupling term between the electronic states. In actual calculation, we use the velocity gauge ($\mathbf{A}\cdot\mathbf{P}$) for the dipole coupling.

Let us first consider a special laser field which is turned on within 20 fs and then held constant. This is a pulse shape used in many theoretical studies on atomic stabilization in superstrong fields [22]. It is similar to a cw laser field but with a reasonable ($\sin^2$) ramp. Figure 3 displays the time evolution of the wave-packet of the molecular system in such a laser field. Initially the molecule is prepared at the $v=14$ vibrational excited state (see the $t=0$ wave packet) and the laser intensity is 5×10^{13} W/cm^2. At such high intensity, the inner part of the molecular wave packet is rapidly dissociated (see $t=10$ and 50 fs graphs). Of particular interest to us, however, is that the outer part of the wave packet is very stably localized and trapped at long times ($t=100$, 150, and 200 fs). Moreover, the trapped part is localized at an internuclear distance ($R_0\approx6.5$ a.u.), independent of time. This is due to the special pulse shape we consider and, as we will see, is generally not the case for a Gaussian pulse. For this simple cw-like laser case, it is interesting to observe that R_0 is precisely the internuclear distance corresponding to the minimum of the uppermost adiabatic potential well (labeled $|g,0\rangle$) at this intensity [c.f. Fig. 1(c)]. It implies the wave packet is trapped by this adiabatic potential well associated with one-photon transition. This is consistent with the results of the complex quasienergy lifetime calculations [c.f. Fig. 2(c)] for the highest-lying vibrational resonances. Therefore in a cw-like field, the molecule, when being prepared in a highly excited vibrational state, can be stably trapped and localized at a stretched internuclear distance determined by the adiabatic potential well around the one-photon crossing. Preparation of H_2^+ molecules in a specific excited vibrational level can be and in fact has been achieved experimentally [6,23]. Extension of this type of experiment to strong probing laser fields will allow the exploration of the laser-induced stabilization and chemical bond-hardening phenomena predicted here and elsewhere [14].

III. MOLECULAR STABILIZATION AND TRAPPING IN INTENSE GAUSSIAN LASER PULSES

Let us now consider nonstationary laser fields; in particular, the Gaussian laser pulses with the envelope $f(t)=\exp[-(1/2)(t/\tau)^2]$, with 2τ being the pulse width. The laser intensity is time dependent for this case and the time-independent results of the complex quasienergies at a single intensity is not directly applicable, though they are still the intrinsic characteristics of the molecule in the fields.

Figure 4 displays the evolution of the wave packet in such a Gaussian pulse. The laser peak intensity is 5×10^{12} W/cm^2 and the pulse width is 100 fs. Again the molecule is initially prepared in the $v=14$ state. The inner part of the wave packet is also dissociated quickly in this case and the outer part, around the peak intensity of the pulse ($t=0$), is primarily trapped at a longer internuclear distance. However, during the trailing edge of

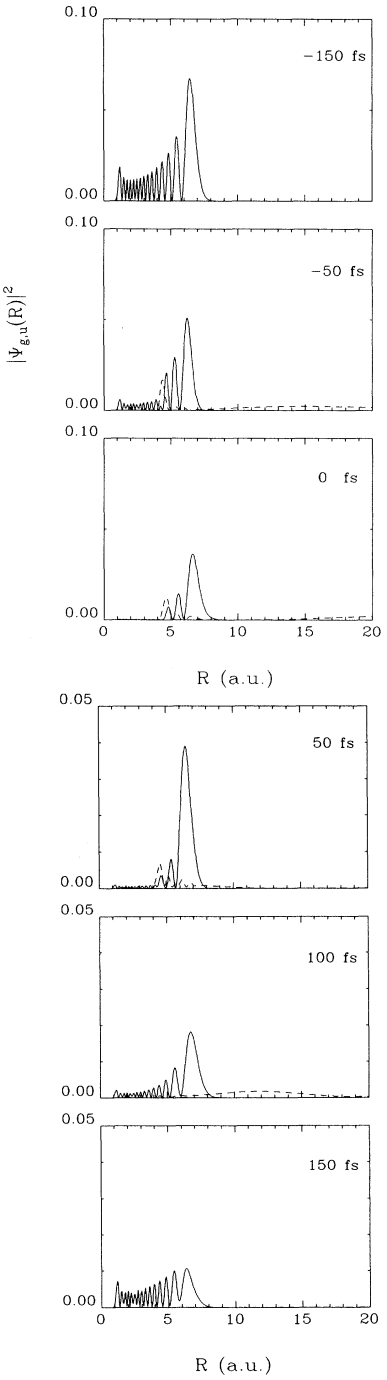

FIG. 4. Time evolution of the wave packet of the $v=14$ highly excited molecule in a Gaussian laser pulse with pulse length 100 fs and peak laser intensity 5×10^{12} W/cm^2. The wave packet is seen to be temporally trapped first at some long distances around the peak intensity and later on becomes redistributed to shorter internuclear distances during the turn-off period of the pulse.

the pulse, the population feeds back to shorter distances (lower vibrational states). The trapped population redistributes among different vibrational states as the time-dependent laser intensity decreases. Evidently this can be attributed to the collapse of the adiabatic potential well with decreasing the laser intensities, i.e., to the fact that the potential well can no longer trap population at large R_0.

Instead of directly looking at the localized wave packet, we may characterize the localization phenomena by defining a local probability, i.e., the integrated probability of finding the molecule between $0 \leq R \leq R_c$. The time dependence of the local probabilities is shown in Fig. 5 for two peak intensities: (a) $I_0 = 5 \times 10^{12}$ W/cm^2, and (b) $I_0 = 5 \times 10^{13}$ W/cm^2, and for $R_c = 15 a_0$. All the other parameters are the same as in Fig. 4. It is seen from Fig. 5(a) that the total local probability decreases, i.e., the molecule dissociated rapidly during the weak-field region (the rising part of the pulse). Around the peak intensity, however, we see a plateau regime (from $t = 0$ to 60 fs), indicating that the total local probability is hardly reduced in spite of the frequency population exchange between the $1s\sigma_g$ and the $2p\sigma_u$ electronic states. This reflects the temporary localization of the molecule, as is also seen in Fig. 4. Note during the falling period of the pulse, the molecule dissociates and the total local probability drops

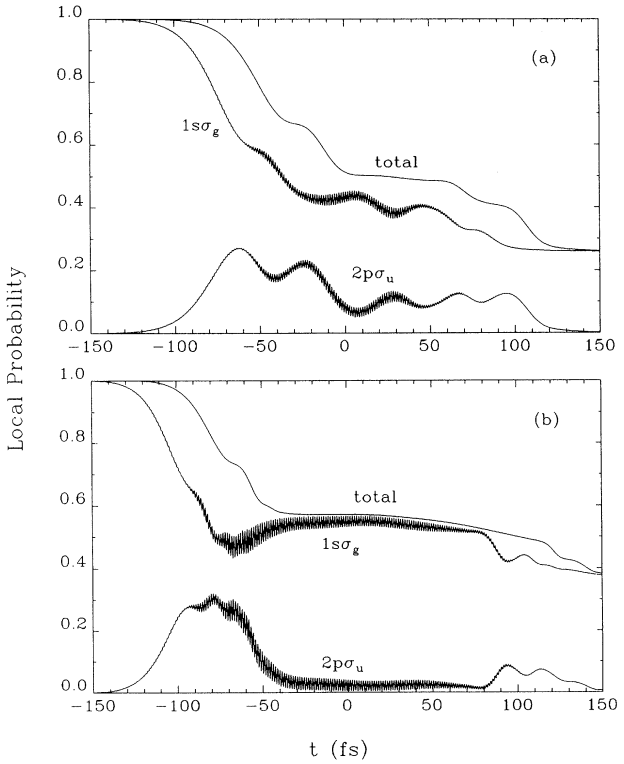

FIG. 5. Local probability (defined as the total population within $R \leq 15$ a.u.) for two laser (peak) intensities, (a) 5×10^{12} W/cm^2, and (b) 5×10^{13} W/cm^2. The laser-pulse width is 100 fs. The plateau represents the stable localization and population trapping regions around the peak intensity.

once again. In particular, the local probability in the $2p\sigma_u$ state is rapidly reduced at the end of the pulse, as this part of the wave packet becomes essentially free in the weak-field limit. On the other hand, the local probability in the $1s\sigma_g$ state is almost unchanged. In other words, this portion is completely localized and trapped after the pulse is over. The trapped population is more than 26%. Therefore the molecule can easily survive both the rising and falling edges of the Gaussian pulse and be substantially trapped.

At higher peak intensity $I_0 = 5 \times 10^{13}$ W/cm^2 [Fig. 5(b)], the local probability decays faster at the early stage of the pulse. Nevertheless the localization is established earlier ($t \approx -50$ fs) and lasts much longer (from $t = -50$ to 100 fs). Also more (37%) population is trapped and localized at the end of the pulse. As a result, the molecule subject to intense laser pulses can be more readily and more stably trapped at high peak intensities than at low ones. This is an unexpected novel intensity-dependent high-field phenomenon. It is a manifestation of the bond-hardening effect in the case of the laser pulse and is qualitatively consistent with the picture obtained from our time-independent Floquet quasienergy calculations [14].

In spite of the slow variation of the total local probability around the peak laser intensity, there is an appreciable dropping in the curve near the trailing edge of the pulse. The reason can be clearly understood from Fig. 6, where the time development of the wave packet in the case of Fig. 5(b) is displayed. While the wave packet is essentially restricted to the short-distance region $R \leq R_c$ ($R_c = 15$ a.u.) after $t = -50$ fs, a large wave packet spreads very slowly into the longer internuclear distance region during the falling edge of the pulse. On the contrary, the inner part population of the localized wave packet again feeds back to shorter-distance region (see the $t = 100$ fs graph). Here trapping manifests itself not only in the final trapped portion after the pulse is over, but in the temporarily trapped part which leaks out slowly with time. The slow leakage effect has recently also been observed by Giusti-Suzor and Mies [17] who referred to it as the "$n = 0$ dissociation" (their $n = 0$ channel is equivalent to our uppermost adiabatic channel $|g,0\rangle$ indicated in Fig. 1). In their case ($\lambda = 248$ nm, peak intensity $I_p = 5 \times 10^{14}$ W/cm^2), the adiabatic curve corresponding to the $|g,0\rangle$ channel is repulsive and lies above the $n = 0$ asymptote. This allows a portion of the trapped wave packet to be pushed above the threshold. In our case (peak intensity $I_p = 5 \times 10^{13}$ W/cm^2 and $\lambda = 775$ nm), however, the uppermost adiabatic potential curve [c.f. Fig. 1(c)] is still attractive around the one-photon avoided crossing region. Thus we might attribute the leakage effect to the fact that the potential well collapses and therefore can no longer support the temporarily trapped large-R wave packet as the laser intensity decreases in the second half of the pulse. This interpretation is consistent with a comparison between the localized wave packet in Fig. 6 and the potential well in Fig. 1(c).

The leakage dissociation manifests itself in the proton kinetic-energy spectrum in Fig. 7 as well, were the low-energy peak represents the slowly leaking trapped frag-

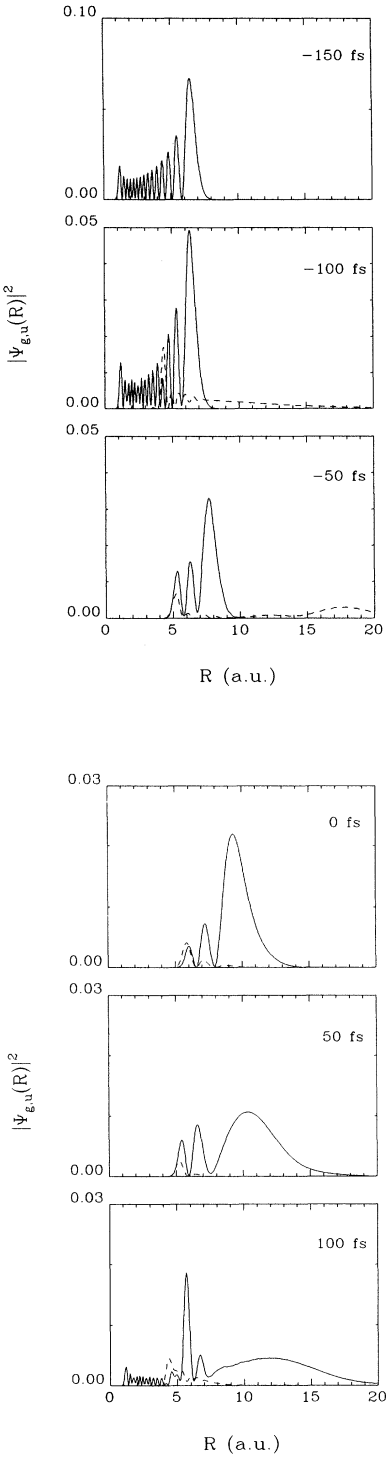

FIG. 6. Time evolution of the wave packet of the $v=14$ highly excited molecule in a 100-fs, 5×10^{13} W/cm^2 Gaussian laser pulse. The distinct feature in this higher intensity case is the prominant temporary localization and trapping at some intermediate internuclear distances and the slow leakage of the wave packet to larger distances. Redistribution of the wave packet to smaller distances near the end of the pulse is also observed, but not as prominent as the lower intensity case (Fig. 4).

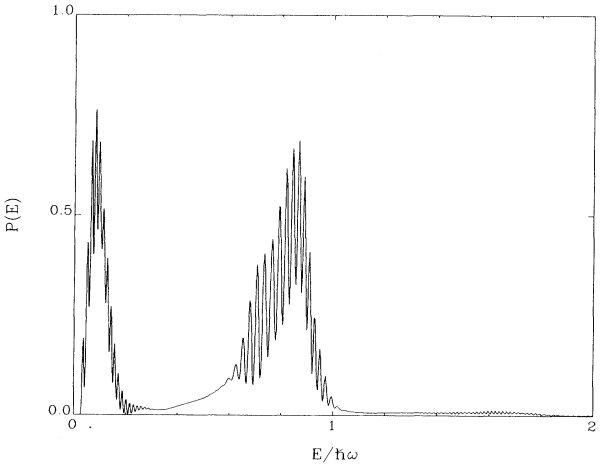

FIG. 7. Proton energy distribution after the pulse is over for the same case as in Fig. 6. The first peak corresponds to the dissociation due to slow leakage of the temporarily localized wave packet, and the second peak is due to the one-photon dissociation.

ment and the high-energy peak corresponds to the dissociation fragment due to one-photon absorption. There is also a weak third peak corresponding to the ATD process. The subpeak structures in the main peaks may be attributed to the quantum-mechanical interference of the momentum space distributions produced at the same laser intensity on the rising and falling edges of the pulse [24]. The leakage dissociation shown in the first peak can be regarded as an indirect evidence of the temporary trapping of the molecule in intense laser pulses. As we never observe similar behavior in our cw-like laser field studies, we attribute it to a pure pulse-shape effect.

The dynamics of the molecular stabilization depends also on the laser pulse length. Figure 8 displays the local

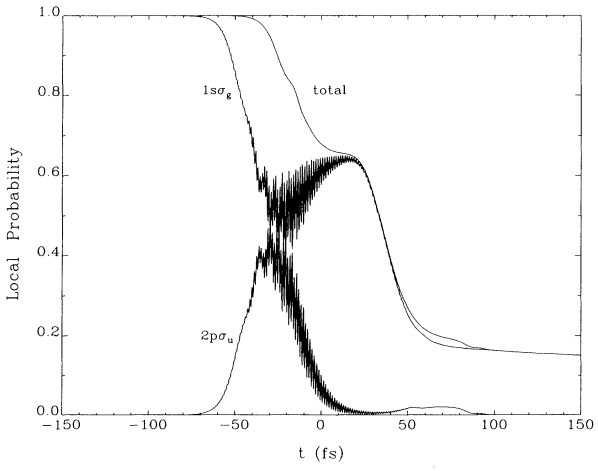

FIG. 8. Time evolution of the local probability of the H_2^+ molecules initially prepared at the $v=14$ state driven by a 50-fs, 5×10^{13} W/cm^2 Gaussian laser pulse. As compared to Fig. 5(b), the shorter pulse considered here appears to trap less population.

probability under the same conditions as in Fig. 5(b) except for a shorter pulse length $2\tau=50$ fs. It is seen by comparison that stable trapping lasts much longer for the 100-fs pulse than for the 50-fs pulse. This is consistent with the intensity dependence of the photodissociation rates shown in Fig. 2. For a longer pulse, there is a longer period of time around the center of the pulse during which the instantaneous intensity is high enough to stabilize the molecule prepared in the high-lying vibrational states. On the other hand, as is shown in Fig. 8, significant dissociation occurs during the long "exponentially decaying" tails of the Gaussian pulse we considered. The total trapped population, therefore, depends delicately not only on the pulse *length* but also on the pulse *shape*. A detailed study of the pulse-length effect on the total bound-state (or trapped) population was given in Ref. [17] using a different, more clear-cut $\sin^4$ pulse. Detailed comparison between the present results and those of Ref. [17] is not straightforward as the pulse shape is different. More detailed study of the pulse-shape effect on the final trapped population will be useful.

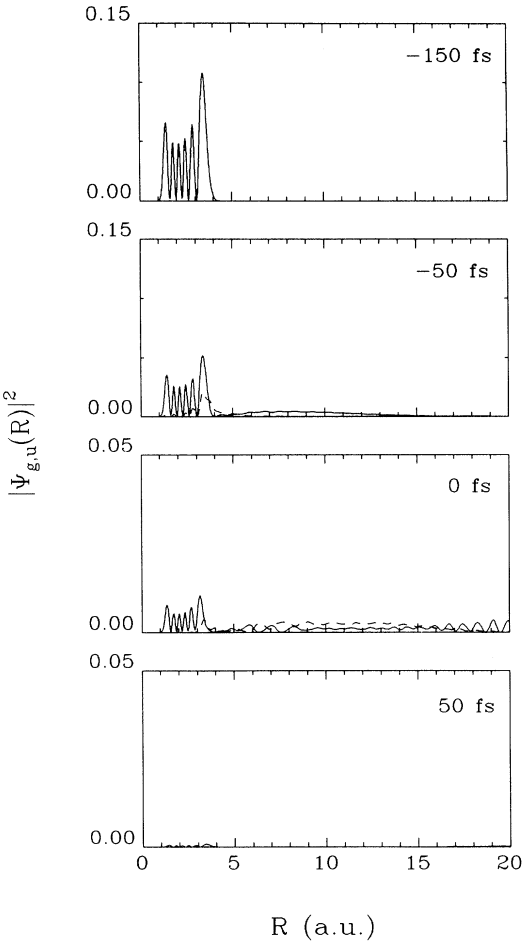

FIG. 9. Time evolution of the wave packet of the low-lying $v=5$ vibrational state in a 100-fs, 5×10^{13} W/cm^2 Gaussian laser pulse, showing rapid dissociation due to the bond-softening effect.

The dynamics of low-lying vibrational states in intense laser pulses is different in many aspects from that of the high-lying ones, such as the $v=14$ state we have discussed. Figure 9 shows the time-dependent wave packet for the molecule initially prepared in the $v=5$ state. The pulse shape is also Gaussian and the pulse width is also 100 fs. The peak intensity is 5×10^{13} W/cm^2. We find that the low-lying state is quickly and almost completely depleted by the same pulse used in Fig. 5(b) and Fig. 7. In contrast to the bond-hardening phenomenon for high-lying states like $v=14$, this is a phenomenon of bond-softening [9]. By comparing with the time-independent results for adiabatic potentials and quasienergies [c.f. Fig. 1(c)], it is evident that the rapid dissociation of the low-lying state is due to the exposure of the $v=5$ state directly to the dissociation continuum resulting from the increasing multiphoton avoided crossing gap between adiabatic potentials with increasing laser intensities. Figure 10 displays the proton energy spectrum after the pulse is over. The first peak here corresponds mainly to the dissociation fragment into the $2p\sigma_u$ electronic state due to the one-photon absorption and the second peak to the dissociation fragment into the $1s\sigma_g$ state due to two-photon absorption. This second peak thus represents the dissociation due to ATD, i.e., to the absorption of one more photon than necessary for dissociation. The spectrum here is also different from that of Fig. 7 where the first peak corresponds to the "leakage dissociation" and no ATD process is appreciable. Similar to that case, the main peaks possess interesting quantum-mechanical interference patterns. In Fig. 10, however, there is no "leakage dissociation" as this is a phenomenon characteristic only for laser-induced stabilization and trapping of high-lying vibrational states. Therefore the population is not trapped even temporarily for this low-lying vibrational state. The behaviors of the low- and high-lying vibrational states are thus dramatically different in intense laser pulses.

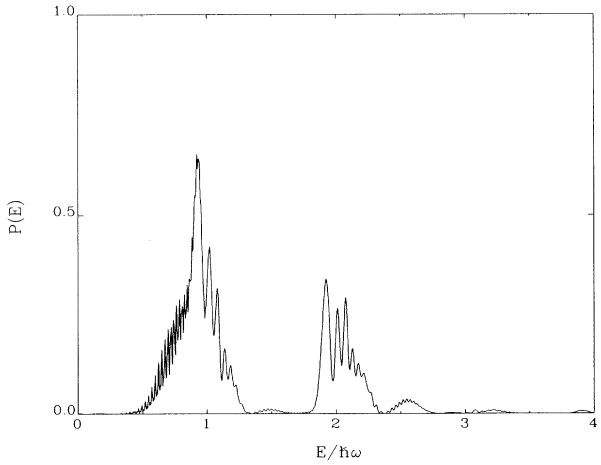

FIG. 10. Proton energy distribution for the case of Fig. 9. The second structured broad peak is due to the ATD process, and the first one to the lowest-order photodissociation.

IV. CONCLUSIONS

In summary, we have studied the MPD-ATD dynamics of the molecular H_2^+ ions in intense cw as well as Gaussian laser fields. The molecules, when initially prepared in high-lying vibrational states, can easily survive both the rising and falling edges of the laser pulse and can be significantly trapped and stabilized. There is a close correlation between the population trapping and the intrinsic intensity-dependent behavior of the vibrational quasienergies at high fields, in particular, the bond-hardening phenomenon. In intense fields, well-separated and nearly decoupled adiabatic potential wells are formed which can support long-lived resonance states and trap significant population. This is exhibited in both the time-independent Floquet rate calculations and the time-dependent wave-packet results. In a cw-like field, the correlation is evidenced by the fact that the wave packet is localized precisely at the adiabatic potential well. In a Gaussian laser pulse, however, laser-induced trapping and localization manifest themselves differently, in spite of the same intensity dependence as in the cw case. First, the trapped population can be redistributed for different internuclear distances as the instantaneous intensity decreases. Second, the wave packet which is temporarily trapped at large distances may slowly leak out for high peak-intensity pulses. The presence of such low-energy fragments in the proton kinetic-energy spectrum is an indication of the temporal trapping. Finally the subpeak structures in the main peaks of the ATD spectrum may be attributed to the quantum interferences of continuum wave packets created at the leading and trailing edges of the pulse [17,24].

The high-intensity effect of the high-lying vibrational states we have discussed is contrary to that of the low-lying states. While the former is more and more stabilized and trapped (bond-hardening), the latter is more and more rapidly dissociated (bond-softening) with increasing laser intensity. They are all due to the strong distortion of the molecular potentials and vibrational structures in intense laser fields.

The population trapping around the three-photon avoided crossing has recently been observed experimentally [20] for $\lambda \approx 775$ nm. In this experiment, a mixture of initial vibrational levels of H_2^+ is created following the multiphoton ionization of H_2 molecules. Since the relative population of the initial vibrational levels was not determined by the experiment, direct comparison of the present calculation with the experimental data is not straightforward. (We also note that in our present study, we do not include the ionization continuum. A recent study by Muller [25] using the length gauge indicates that the neglect of competition with photoionization can be justified.) While our previous study [14] explored the molecular trapping in different potential wells ("multiple-well trapping"), the present work focuses on the trapping at the one-photon avoided crossing of the vibrationally excited molecules and on the pulse effect on the trapping dynamics. This has not been explored experimentally. Preparation of H_2^+ molecules in a specific excited vibrational level by different experimental techniques [6,23] may provide a useful test of the present theoretical results and also facilitate direct comparison of the present theory with experiments.

ACKNOWLEDGMENTS

This work was partially supported by the Division of Chemical Sciences, Office of Basic Energy Sciences of the U.S. Department of Energy. Acknowledgment is also made to CRAY Research Inc. for the access to CRAY-YMP supercomputer facilities at NCAR (Boulder, CO).

[1] N. Bloembergen and E. Yablonovitch, Phys. Today **31**, 23 (1978); P. A. Schulz, Aa. S. Sudbo, D. J. Krajnovich, H. S. Kwok, Y. R. Shen, and Y. T. Lee, Annu. Rev. Phys. Chem. **30**, 311 (1979).

[2] See, for example, V. S. Letokhov, *Nonlinear Laser Chemistry* (Springer, New York, 1983); in *Photoselective Chemistry,* edited by J. Jortner, R. D. Levine, and S. A. Rice, Advances in Chemical Physics Vol. 47 (Wiley, New York, 1981); *Advances in Multiphoton Processes and Spectroscopy,* edited by S. H. Lin (World Scientific, Singapore, 1984, 1986, 1988).

[3] S. I. Chu, J. Chem, Phys. **75**, 2215 (1981).

[4] S. I. Chu, C. Laughlin, and K. K. Datta, Chem. Phys. Lett. **98**, 476 (1983).

[5] C. Laughlin, K.-K. Datta, and S. I. Chu, J. Chem. Phys. **85**, 1403 (1986).

[6] A. Carrington and J. Buttenshaw, Mol. Phys. **44**, 267 (1981).

[7] A. D. Bandrauk and M. L. Sink, J. Chem. Phys. **74**, 1110 (1981); A. D. Bandrauk and G. Turcotte, J. Phys. Chem. **87**, 5098 (1983).

[8] For a recent review in this field, see R. R. Freeman and P. H. Bucksbaum, J. Phys. B **24**, 325 (1991).

[9] P. H. Bucksbaum, A. Zavriyev, H. G. Muller, and D. W. Schumacher, Phys. Rev. Lett. **64**, 1883 (1990); B. Yang, M. Saeed, L. F. Dimauro, A. Zavriyev, and P. H. Bucksbaum, Phys. Rev. A **44**, R1458 (1991).

[10] C. Cornaggia, D. Normand, J. Morellec, G. Mainfray, and C. Manus, Phys. Rev. A **34**, 207 (1986); J. W. J. Verschuur, L. D. Noordam, and H. B. van Linden van den Heuvell, Phys. Rev. A **40**, 4383 (1988).

[11] S. W. Allenodorf and A. Szöke, Phys. Rev. A **44**, 518 (1991); H. Helm, M. J. Dyer, and H. Bissantz, Phys. Rev. Lett. **67**, 1234 (1991); T. S. Luk and C. K. Rhodes, Phys. Rev. A **38**, 6180 (1988).

[12] C. Cornaggia, J. Lavancier, D. Normand, J. Morellec, P. Agostini, J. P. Chambaret, and A. Antonetti, Phys. Rev. A **44**, 4499 (1991); G. N. Gibson, R. R. Freeman, and T. J. McIlrath, Phys. Rev. Lett. **67**, 1230 (1991).

[13] See, for example, (a) A. Giusti-Suzor, X. He, O. Atabek, and F. H. Mies, Phys. Rev. Lett. **64**, 515 (1990); (b) X. He, O. Atabek, and A. Giusti-Suzor, Phys. Rev. A **42**, 1585 (1990).

[14] G. Yao and S. I. Chu, Chem. Phys. Lett. **197**, 413 (1992).

[15] S. I. Chu, J. Chem. Phys. **94**, 7901 (1991).
[16] S. I. Chu, Chem. Phys. Lett. **167**, 155 (1990).
[17] A. Giusti-Suzor and F. H. Mies, Phys. Rev. Lett. **68**, 3869 (1992).
[18] For reviews on complex-scaling Floquet Hamiltonian methods, see S. I. Chu, Adv. At. Mol. Phys. **31**, 197 (1985); Adv. Chem. Phys. **73**, 739 (1989).
[19] C. C. Marston and G. G. Balint-Kurti, J. Chem. Phys. **91**, 3571 (1989).
[20] P. H. Bucksbaum (private communication); A. Zavriyev, P. H. Bucksbaum, J. Squier, and F. Saline, Phys. Rev. Lett. **70**, 1077 (1993).
[21] M. D. Feit, J. A. Fleck, Jr., and A. Steiger, J. Comput. Phys. **47**, 412 (1982).
[22] See, e.g., K. C. Kulander, K. J. Schafer, and J. L. Krause, Phys. Rev. Lett. **66**, 2601 (1991); V. C. Reed, P. L. Knight, and K. Burnett, *ibid.* **67**, 1415 (1991).
[23] A. Carrington, J. Buttenshaw, and R. A. Kennedy, Mol. Phys. **48**, 775 (1983).
[24] See, e.g., J. N. Bardsley, A. Szoke, and M. J. Comella, J. Phys. B **21**, 3899 (1988); V. C. Reed and K. Burnett, Phys. Rev. A **43**, 6217 (1991).
[25] H. G. Muller, in *Coherence Phenomena in Atoms and Molecules in Strong Laser Fields,* edited by A. D. Bandrauk and S. C. Wallace (Plenum, New York, 1992), p. 89.